J Mater Sci (2008) 43:6289–6295
DOI 10.1007/s10853-008-2892-7

Gas phase hydrogenation reaction using a 'metal nanoparticle–polymer' composite catalyst

Kaushik Mallick · Kartick Mondal · Mike Witcomb · Mike Scurrell

Received: 17 February 2008 / Accepted: 22 July 2008 / Published online: 13 August 2008

Abstract A facile synthesis route is described here for the preparation of a poly (anthranilic acid)-palladium nanoparticle composite material by polymerization of anthranilic acid (AA) monomer using palladium acetate (PA) as the oxidant. It was found that oxidative polymerization of AA leads to the formation of poly-AA (PAA), while the reduction of PA results in the formation of palladium nanoparticles with an average size of ~ 2 nm. The palladium nanoparticles were uniformly dispersed and highly stabilized within the macromolecular matrix resulting in a uniform metal–polymer composite material. The resultant composite material was characterized by means of different techniques, such as IR and Raman spectroscopy, which yielded information about the chemical structure of polymer, whereas electron microscopy images provided information concerning the morphology of the composite material and the distribution of the metal particles in the composite material. The composite material was tested as a catalyst for ethylene hydrogenation reaction and showed a catalytic activity at higher temperatures.

K. Mallick (✉)
Advanced Materials Division, Mintek, Randburg 2125, South Africa
e-mail: Kaushikm@mintek.co.za

K. Mondal · M. Scurrell
Molecular Sciences Institute, School of Chemistry, University of the Witwatersrand, Private Bag 3, WITS, Johannesburg 2050, South Africa

M. Witcomb
Electron Microscope Unit, University of the Witwatersrand, Private Bag 3, WITS, Johannesburg 2050, South Africa

Introduction

Hybrid composites based on polymer–metal nanoparticles with nano- or micro-dimensions are an area of considerable scientific and technical interest since they offer the opportunity to material scientists to synthesize a broad range of promising new materials [1]. There have been a variety of attempts reported in the literature to make nanoparticle–polymer composite materials. Overall, we note four different approaches utilized to date. The first technique [2] consists of the preparation of metal nanoparticles in the matrix. This is done by the reduction of metal salts dissolved in the polymer matrix. The second method [3] consists of polymerizing the matrix around the preformed metal nanoparticles. The third approach [4] has involved the blending of preformed nanoparticles into a pre-synthesized polymer. The fourth procedure [5] is the most desirable approach to achieve an intimate contact between the metal and the polymer, and it involves the blending of a monomer and a metal salt. The choice of the metal salt and the monomer should be such that the metal salt can oxidize the monomer to form a polymer while the reduction of the metal salt can produce metal nanoparticles.

Metal nanoparticles of different sizes and shapes can be combined with polymers to produce a host of composites having interesting physical properties and important potential applications. Depending on the synthesis techniques used and the characteristics of the inorganic materials, the ultimate properties of the resulting composite can be controlled [1].

Gold [6, 7], copper [8], platinum [9], and palladium [10] nanoparticles have been successfully incorporated into polyaniline or substituted polyaniline. Copper, cobalt, and nickel particles embedded in polyaniline matrices have also been prepared by a polyol process in which the reduction of

a precursor and polymerization are achieved in one step at 180 °C [11].

We have demonstrated a facile in situ synthesis route for a Au-polyaniline composite in which 10–50 nm sized gold nanoparticles are decorated on micro-size polyaniline balls [12]. We have successfully produced highly dispersed copper nanoparticles (2.5–10 nm of which 50% of the Cu nanoparticles are within the size range 2–4 nm) in a thin film of poly- (*o*-toluidine) [13]. A metal–poly (*o*-aminophenol) composite [14] has been successfully produced when 2–4 nm diameter palladium nanoparticles were incorporated as the metallic component of the composite material.

In the present communication, we report on a simple, one pot chemical synthesis route for the preparation of a PAA and palladium nanoparticle composite material in which the palladium particles are embedded and totally encapsulated in the polymer matrix. An in situ method of preparation for the composite material is particularly attractive from a synthetic point of view since both the components of the composite material have ample scope for intimate contact. In the case of a polymer and metal nanoparticle composite material, the process starts from the monomer (in the case of polymer) and the ionic state (in the case of metal particle). Thus, the molecular level interaction between the host (polymer) and the guest (metal particle) can yield interesting physical properties and significant potential applications. The results from our laboratory reported earlier were limited to the milligram scale since scaling-up sometimes resulted in reproducibility problems, whereas, the present communication presents a gram-scale synthesis approach with good reproducibility. The composite was used as a catalyst for the hydrogenation reaction and showed activity at higher temperatures. The mechanistic approach of the synthesis, the optical and the micro-analytical characterization of this kind of composite material, and the behavior of this material as a catalyst will be discussed here.

Experimental

Materials

Unless otherwise indicated, all the chemicals were of analytical grade and were used as received. Toluene was obtained from Merck, and Pd-acetate was sourced from Next *Chemica*. A stock solution of Pd-acetate (10^{-2} mol dm^{-3}) was prepared in toluene. Anthranilic acid was purchased from BDH (London).

Procedure for the synthesis of composite material

In a typical experiment, 1.32 g of anthranilic acid was dissolved in 25 mL of methanol in a 50 mL conical flask under continuous stirring conditions. Fifteen milliliters of a previously prepared stock solution of Pd-acetate in toluene was added drop by drop to the first solution. Initially, a dark brown colorization was observed followed by a light pink precipitation. The entire procedure was carried out at room temperature and under continuous stirring conditions. Subsequently, the solution was allowed to stand at rest for 10 min during which time all the precipitated material deposited at the bottom of the flask. TEM specimens were prepared by pipetting the deposited material onto a lacey carbon-coated nickel grid. The rest of the solution was then filtered, and a small portion of the solid mass was used for the IR and Raman analyses.

Characterization techniques

The solid sample was used for infrared spectra analysis, in the range 4000–700 cm^{-1}, using a Perkin-Elmer 2000 FT-IR spectrometer operating at a resolution 4 cm^{-1}. The sample was deposited in the form of a thin film on a NaCl disk.

Raman spectra of the solid sample were acquired using the green (514.5 nm) line of an argon ion laser as the excitation source. Light dispersion was undertaken via the single spectrograph stage of a Jobin-Yvon T64000 Raman spectrometer. Power at the sample was kept very low (0.73 mW), and the laser beam diameter at the sample was ~ 1 μm.

Transmission electron microscopy (TEM) studies of the samples were carried out at an accelerating voltage of 120 kV using a Philips CM200 TEM equipped with a LaB_6 source. A super ultra-thin windowed energy dispersive X-ray spectrometer (EDS) attached to the TEM was used to determine the chemical composition of the samples. TEM specimens were prepared by pipetting 2 μL of colloid solution from the bottom of the flask onto lacey, carbon-coated, nickel TEM grids. Differential scanning calorimetric (DSC) study was carried out on a Setaram microcalorimeter using a scan rate of 10° per min under nitrogen atmosphere.

Reactivity measurements

The selective hydrogenation reaction was performed at atmospheric pressure by passing a continuous gaseous feed containing pure ethylene and hydrogen (C_2H_4/H_2 mol ratio = 3.05, total flow of feed gas = 77 mL/min) over the catalyst (50 mg) packed in a fixed-bed quartz micro-reactor, provided with a thermocouple in the catalyst bed, at different temperatures. After attaining the reaction steady state, the reaction products were analyzed by a gas chromatograph with a flame ionization detector using a Porapak Q column. The catalyst was studied in its as-prepared state.

Since only hydrocarbon products are detected by the flame ionization detector, the selectivity and conversion thus were based solely on analysis of the hydrocarbons.

Results and discussions

IR and Raman spectroscopic techniques were used to investigate the optical behavior of the solid sample. The IR spectrum of the resultant compound is presented in Fig. 1. The band at 1510 cm^{-1} can be assigned to the C=C stretching vibration of the benzenoid rings while the peak at 1385 cm^{-1} is attributed to the >C=O stretching vibration of COO^- groups. A broad band with a peak position at 1650 cm^{-1} can be attributed the C=C stretching vibration of the quinoid rings. The band at 1245 cm^{-1} is derived from the C–N stretching vibration. The peaks at 1134 and 1042 cm^{-1} correspond to the aromatic C–H in-plane bending vibration. The aromatic out-of-plane C–H deformation vibrations correspond to the band at 800 cm^{-1} and this indicates the presence of the 1–4 substituted benzene rings. The bands at 3439, 3356, and 3222 cm^{-1} correspond to the N–H stretching vibration, whereas the broad band at 2900 cm^{-1} results from the aromatic C–H stretching vibration. Overall, the IR spectrum indicates that the resultant material is the polymeric form of AA with the combination of the benzenoid and the quinoid forms of structure.

Figure 2 represents the typical Raman spectrum obtained from the synthesized material. The bands between 1100 and 1700 cm^{-1} are sensitive to the PAA oxidation state. The band at 1168 cm^{-1} corresponds to the CH benzene deformation mode indicating the presence of quinoid rings. The C–C deformation band of the benzenoid ring is observed at

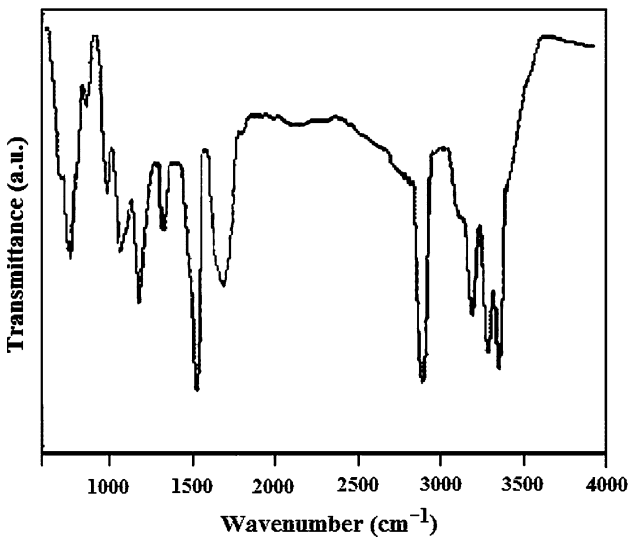

Fig. 1 Fourier transform IR spectrum of the composite material

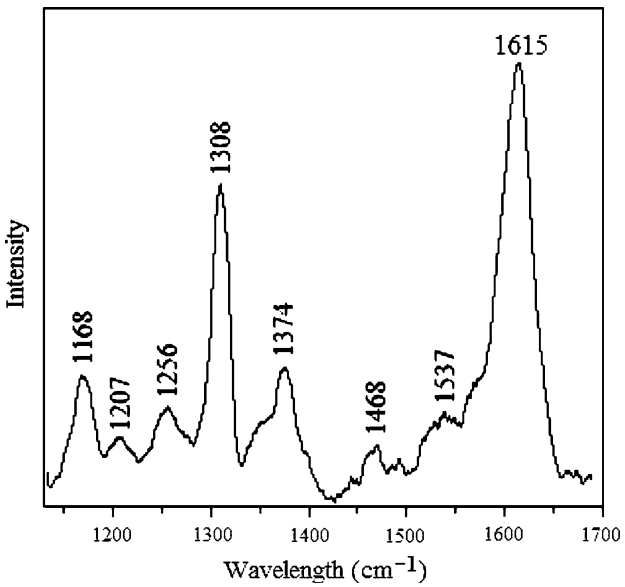

Fig. 2 The Raman spectrum obtained from the composite material

1615 cm^{-1}. A small peak at 1537 cm^{-1} corresponds to the N–H bending deformation band of protonated amine. Two intense peaks at 1308 and 1374 cm^{-1} correspond to C–$N^{\bullet+}$ stretching modes of the delocalized polaronic charge carriers. Another small band at 1468 cm^{-1} corresponds to C=N stretching mode of the quinoid units. The band at 1256 cm^{-1} can be assigned to the C–N stretching mode of the polaronic units whereas the band at 1207 cm^{-1} corresponds to C–N stretching mode due to the single bonds.

The IR and Raman spectra of the resultant material indicate that the polymer is in a partially oxidized form with the presence of both benzenoid and quinoid units in the structure.

The resultant material was studied by TEM to document the morphology of the polyanthranilic acid and to determine the fate of the palladium acetate during the reaction. Figure 3a shows the general morphology of the resultant material revealing that the small agglomerated polymer units (1–2 μm) form a chain-like structure. Figure 3b is the higher magnification TEM image of a single agglomerated polymer unit showing that it takes a thin film-like appearance. High magnification images, Fig. 4a–c, and stereo images reveal evenly distributed dark spots of diameter about 2 nm throughout the thin film-like structure. EDX analyses obtained from the electron beam being focused onto the dark spots indicated that these spots were palladium.

EELS mapping for the distribution of palladium in the composite material has provided unambiguous confirmation that the dark spots are palladium. This is most clearly illustrated in Fig. 5 where a small portion of the polymer composite was isolated such that portions of the thin films

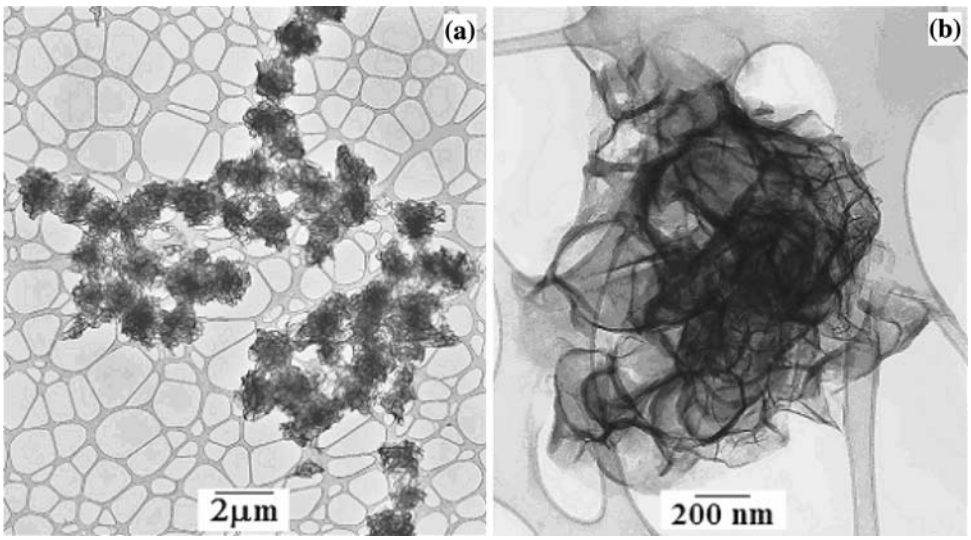

Fig. 3 Low magnification TEM images showing (**a**) the small agglomerated polymer units forming a chain-like structure, (**b**) thin film-like appearance of a polymer unit

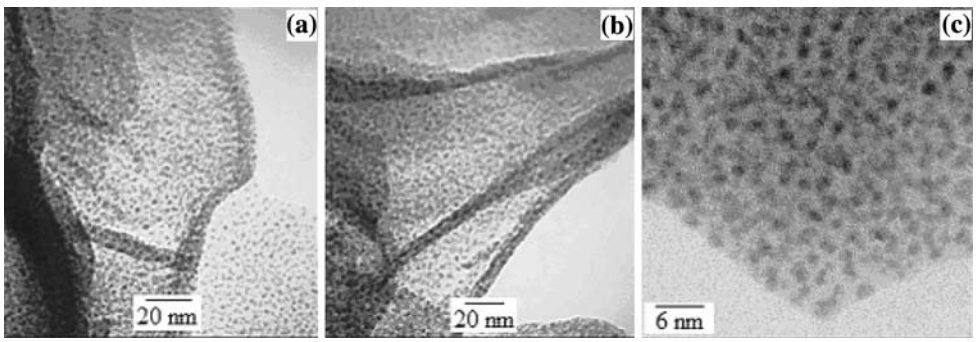

Fig. 4 Higher magnification TEM images of the polymer composite, the dark spots being palladium nanoparticles

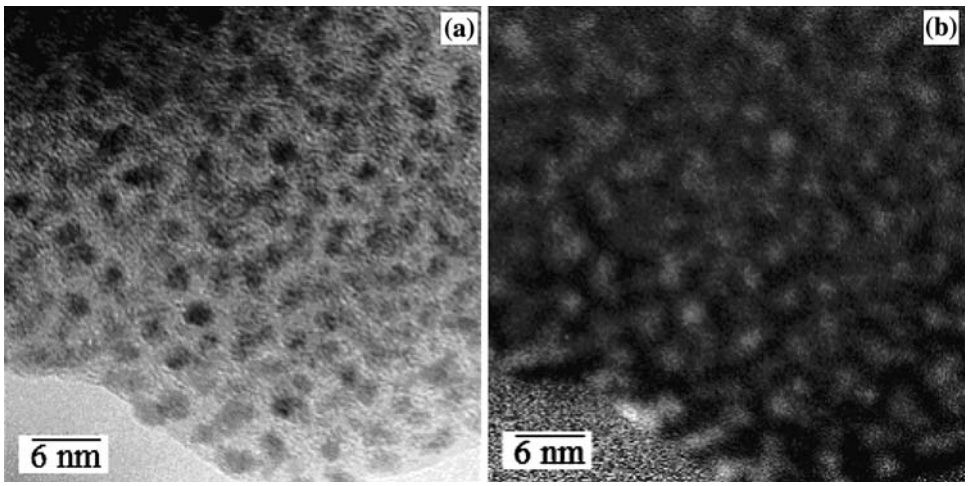

Fig. 5 (**a**) Zero-loss image of the polymer-nanoparticle composite, (**b**) Pd-$N_{2,3}$ edge jump-ratio image of the area shown in (**a**). All of the dark regions in (**a**) can clearly be identified as palladium nanoparticles

were not overlapping. Figure 5a is a zero-loss image of the composite. This is an energy filtered image such that it is only derived from electrons which have retained the beam energy when passing through this thin sample. This image contains no useful micro-analytical information. In contrast, Fig. 5b is a palladium map from the same region. This Pd jump-ratio image was obtained by dividing the Pd-$N_{2,3}$ post-edge loss image (an image derived from the signal from an energy window placed just above the ionization energy of Pd N shell X-rays, the signal being the sum of the background signal at this position which contains no micro-analytical information, and the signal resulting from electrons that lost energy by generating Pd N shell X-rays) by the pre-edge image (an image derived from the signal from an energy window placed just before the ionization energy of Pd N shell X-rays, this image

being a background image). Comparing the zero-loss and jump-ratio image, it can be seen that the dark areas in Fig. 5a correspond to all of the approximately 2 nm diameter Pd particles mapped in Fig. 5b. The formation of metallic palladium particles are also confirmed by XPS and XRD measurement.

Anthranilic acid falls under the substituted aniline group of compounds in which the carboxylic group (–COOH) is attached at the *ortho* position of the aniline. A wide variety of methods have been applied to the preparation of polyaniline or substituted polyaniline type compounds by the oxidative polymerization from their monomer. During the polymerization process, each step is involved with a release of an electron [15]. Those electrons can then reduce the palladium acetate salt (Pd^{2+}) to Pd (0). Spectroscopic analysis confirmed that the –COOH substituted aniline oxidation product has a head-to-tail (–N–Ph–N–Ph–)-like arrangement rather than a head-to-head (–Ph–N=N–Ph–) type. Stereo TEM images have indicated that the palladium nanoparticles are highly dispersed and encapsulated in the PAA matrix. For further confirmation, the Pd–PAA composite was used as the catalyst for ethylene hydrogenation reaction.

Figure 6 shows the temperature-dependent activity and selectivity graph for the ethylene hydrogenation reaction when the palladium–PAA composite material was used as the catalyst. The ethylene conversion was found only to start at about 95 °C, Fig. 6. While only 4% ethane was produced during the reaction between ethylene and hydrogen at 100 °C about 30% ethylene conversion was achieved at

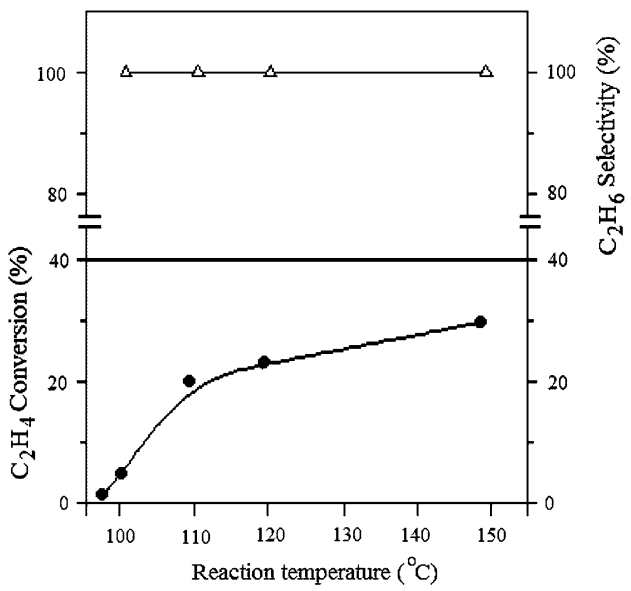

Fig. 6 Time-of-stream activity over the palladium-polyanthranilic acid catalyst in the hydrogenation of ethylene at 110 °C [H_2/C_2H_4 = 3.05; GHSV = 71148 cm^3 g^{-1} h^{-1}, amount of Pd-PAA composite used = 0.05 g]

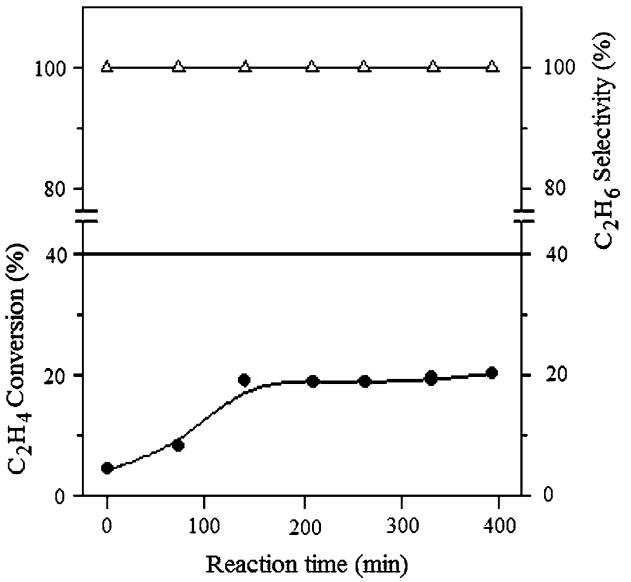

Fig. 7 Effect of temperature on the performance of the palladium–polyanthranilic catalyst in the hydrogenation of ethylene [H_2/C_2H_4 = 3.05, amount of Pd–PAA composite used = 0.05 g, GHSV = 71148 cm^3 g^{-1} h^{-1}]

150 °C. This demonstrates that the hydrogenation reaction is thermodynamically favorable at higher temperatures. Figure 7 shows the time-on-stream activity and selectivity of the palladium-based polymer composite material as a catalyst for the reaction between ethylene and hydrogen. A conversion of 20.5% of ethylene has been obtained for the selective hydrogenation reaction at 110 °C. This reaction occurs at a space velocity of 71148 cm^3 g^{-1} h^{-1}. While only a small amount of conversion was found during the initial reaction period (2 h), subsequently the hydrogenation reaction activity increased with time.

The softening (glass transition) [16] behavior of polyaniline and dopped polyaniline has been found in the range 75–94 °C [17] and as in the present case the polymer is the derivative of polyaniline so it is expected that a similar event could be happen near by temperature zone. In our system poly (*ortho*-amino benzoic acid) shows the onset of glass transition temperature at 85 °C (DSC thermograph not shown). At this stage, the metal–polymer binding energy is not so effective and the palladium particles start to migrate from the interior of the composite to the surface of the polymer. When some of the palladium particles are on the surface of the polymer the reactant species (ethylene and hydrogen) come in contact with them and they show catalytic activity. During the movement of the particles their possible agglomeration cannot be ruled out. The schematic diagram, Fig. 8, illustrates the process. When a considerable number of active sites become available on the surface of the polymer the system will show reasonable activity as a catalyst. To confirm the above explanation the

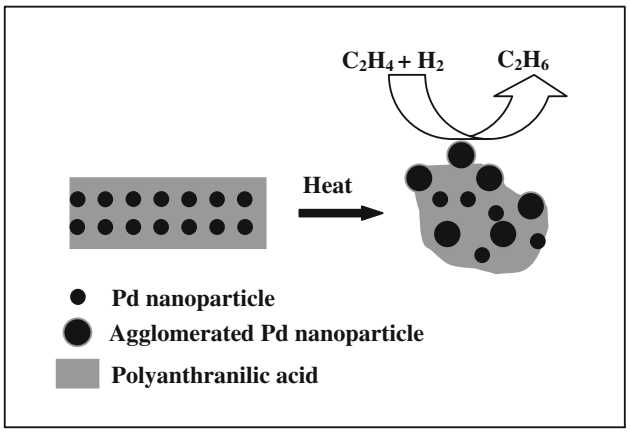

Fig. 8 Schematic diagram of the migration and agglomeration of the palladium nanoparticles as a result of the thermal treatment

used catalyst sample (composite) was examined by TEM. Comparing the zero-loss image, Fig. 9a, and the Pd jump-ratio image, Fig. 9b, it can be seen that the dark areas in Fig. 9a correspond to all of the Pd particles mapped in Fig. 9b. Clearly, a massive migration and agglomeration of the palladium particles had occurred. A higher magnification TEM image, Fig. 10, clearly illustrates the agglomeration and clustering of the palladium particles. The darker regions, two are outlined with white circles in the inset for example, are the palladium particles that at some stage during the thermal treatment are no longer encapsulated by the polymer and thus become active sites of the catalyst.

Conclusions

The results demonstrate a single step synthetic route for the preparation of palladium–poly (anthranilic acid) composite material in which palladium acetate and anthranilic acid

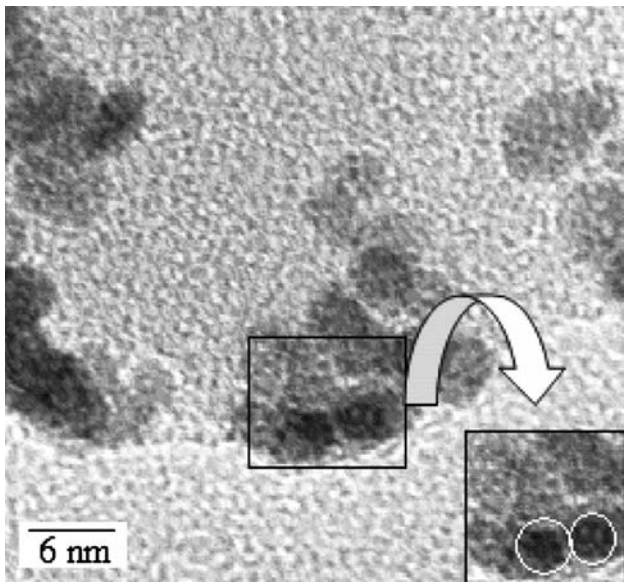

Fig. 10 TEM image reveals the agglomeration and clustering of the palladium particles. The darker regions (inset: surrounded by white circles) are the active sites of the catalyst that are created during the thermal treatment at the time of reaction. The composite is lying on top of the carbon support film

were utilized as the precursor. The presence of both the benzenoid and the quinoid form in the polymer, as evidenced by IR and Raman spectra, indicates that the polymer is not in the fully oxidized form. TEM and EELS analyses showed that the palladium nanoparticles are uniformly dispersed in the polymer matrix with a uniform size distribution of $\sim$2 nm. The response of the ethylene hydrogenation reaction using the composite as the catalyst has confirmed the structural arrangement within the fabricated composite as well as its response to heating. Superstructured nanomaterials such as described here have some novel properties which are technologically useful in different sensor applications and the research on this

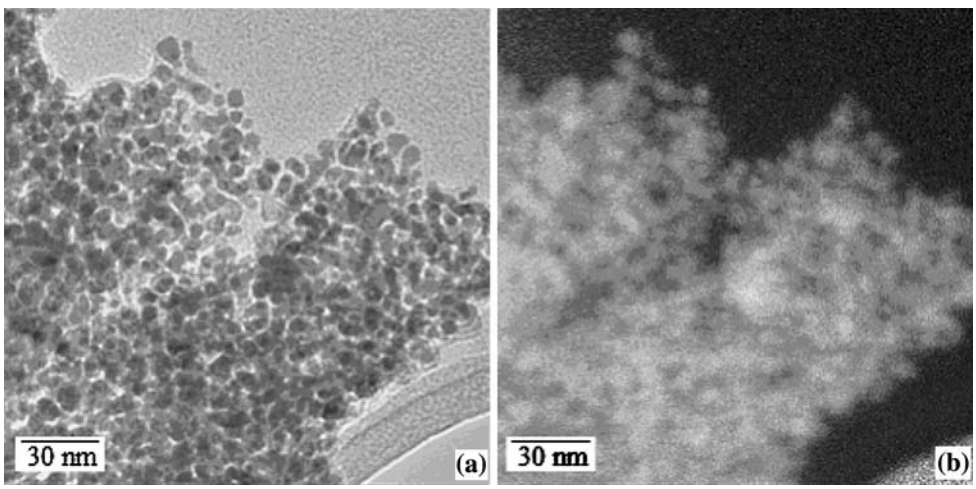

Fig. 9 (**a**) Zero-loss image of a used polymer composite at the end of the reaction, (**b**) Pd-$N_{2,3}$ edge jump-ratio image of the area shown in (**a**). All of the dark regions in (**a**) can clearly be identified as palladium particles

system which is currently in progress will be addressed in the future publications.

References

1. Gangopadhyay R, De A (2000) Chem Mater 12:608
2. Selvan ST, Spatz JP, Klok HA, Möller M (1998) Adv Mater 10:132
3. Lee J, Sundar VC, Heine JR, Bawendi MG, Jensen KF (2000) Adv Mater 12:1102
4. Corbierre MK, Cameron NS, Sutton M, Mochrie SGJ, Lurio LB, Rühm A, Lennox RB (2001) J Am Chem Soc 123:10411
5. Mallick K, Witcomb MJ, Scurrell MS (2007) Phys Status Solidi (RRL) 1:R1
6. Dai X, Tan Y, Xu J (2002) Langmuir 18:9010
7. Kinyanjui JM, Hatchett DW, Smith JA, Josowicz M (2004) Chem Mater 6:3390
8. Vijaya Kumar R, Mastai Y, Diamant Y, Gedanken A (2001) J Mater Chem 11:1209
9. O'Mullane AP, Dale SE, Macpherson JV, Unwin PR (2004) Chem Commun 1606
10. Hasik M, Wenda E, Bernasik A, Kowalski K, Sobczak JW, Sobczak E, Bielańska E (2003) Polymer 44:7809
11. Deschamps A, Lagier JP, Fievert F, Aeiyach S, Lacaze PC (1992) J Mater Chem 2:1213
12. Mallick K, Witcomb MJ, Dinsmore A, Scurrell MS (2005) Macromol Rapid Commun 26:232
13. Mallick K, Witcomb MJ, Scurrell MS (2006) Eur Polym J 42:670
14. Mallick K, Witcomb MJ, Dinsmore A, Scurrell MS (2006) J Mater Sci 41:1733. doi:10.1007/s10853-006-3950-7
15. Mallick K, Witcomb MJ, Scurrell MS (2006) Gold Bull 39:136
16. Panshin BI, Perov BV, Fedorenko AG (1971) Mech Comp Mater 7:159
17. Kazim S, Ali V, Zulfequar M, Haq MM, Husain M (2007) Curr Appl Phys 7:68